



## Impact of Nano-Pomegranate Seed Oil on the Expression of TLR2 and TLR4 Genes in A549 Cells Sensitized with *Alternaria alternata* Cellular Extract

Seyed Mehdi Joghataei<sup>1</sup>, Donya Nikaein<sup>1,2\*</sup>, Ghazale Arshadi Nezhad<sup>1</sup>,  
Alireza Khosravi<sup>1,2</sup>, Iradj Ashrafi Tamai<sup>1</sup>

<sup>1</sup> Department of Microbiology and Immunology, Faculty of Veterinary Medicine, University of Tehran, Tehran, Iran.

<sup>2</sup> Mycology Research Center, Faculty of Veterinary Medicine, University of Tehran, Tehran, Iran.

### ARTICLE INFO

#### Article type:

Research Article

#### Article history:

Received: 16 Sep 2024

Revised: 02 Oct 2024

Accepted: 23 Oct 2024

Published: 04 Nov 2024

#### Keywords:

*Alternaria alternata*,  
Pomegranate seed oil,  
Nano-emulsions, asthma,  
Anti-inflammatory.

### ABSTRACT

**Background:** Allergies impact nearly 30% of the world's population, with fungi being remarkable contributors to allergic sensitivity. Exposure to fungi allergens can trigger allergic reactions and severe asthma has been linked to hypersensitivity to fungi such as *Aspergillus* and *Alternaria* spp. *Alternaria alternata*, a common allergen in respiratory allergic diseases, releases proteases that initiate Th2 responses, causing inflammatory cytokine production. Given the anti-inflammatory properties of Pomegranate Seed Oil (PSO) and the potential of Nano-emulsions (NEs) to enhance drug delivery, this study investigates the impact of PSO-loaded NEs on TLR2 and TLR4 gene expression in A549 cells sensitized with *A. alternata* extract (ALT).

**Methods:** *A. alternata* (ATCC 6663) was cultured and processed to obtain a cytosolic extract, with protein content measured using the Bradford method. Using a Soxhlet apparatus, PSO was extracted from cleaned, dried seeds and analyzed by gas chromatography. Alginate nanospheres containing PSO were prepared through a modified water-in-oil emulsification method and characterized for particle size, polydispersity index, and zeta potential. A549 cells were cultured and treated with various ALT, PSO, and PSO-loaded NEs combinations. Following treatment, RNA was extracted, and real-time RT-PCR was conducted to analyze TLR2 and TLR4 gene expression.

**Results:** All treatment groups showed an increase in TLR2 gene expression compared to the control, with the ALT combined with PSO (P+ALT) causing the highest increase at 4.82-fold. Free PSO (P) and free NEs (NP) resulted in 3.92-fold and 2.93-fold increases, respectively, while the ALT and PSO-loaded NEs (NP+ALT) led to 2.26-fold and 2.50-fold increases. For TLR4 gene expression, the ALT treatment increased expression by 2.29-fold, but treatments containing PSO (P, P+ALT, NP+ALT) reduced TLR4 expression, with P+ALT and NP+ALT causing 0.45-fold and 0.61-fold decreases.

**Conclusion:** The study confirms that herbal extracts like PSO selectively upregulate TLR2 and downregulate TLR4, suggesting targeted therapeutic potential in inflammation and immune modulation. PSO-loaded NEs demonstrated superior anti-inflammatory effects, supporting their development for treating inflammatory diseases and warranting further research into their molecular mechanisms and therapeutic applications.

- **Please cite this paper as:** Joghataei SM, Nikaein D, Arshadi Nezhad G, Khosravi A, Ashrafi Tamai I. Impact of Nano-Pomegranate Seed Oil on the Expression of TLR2 and TLR4 Genes in A549 Cells Sensitized with *Alternaria alternata* Cellular Extract. *J Med Bacteriol.* 2024; **12** (4): pp.17-30.

## Introduction

Allergies are a type of immune response that affects nearly 30% of the world's population. Fungi are well-known as one of the causes of allergic sensitivity (1, 2). Different allergic reactions can occur in atopic people when exposed to fungi allergens. Severe asthma is linked to hypersensitivity to fungi like *Aspergillus* and *Alternaria* spp. according to research (1, 3). The most prevalent fungus in allergic diseases is *Alternaria alternata*, (4) a saprophytic species with global distribution (2,5,6). *A. alternata* releases proteases that may act as a stimulus to start the Th2 response by producing TSLP. TSLP is a cytokine similar to IL-4, produced by epithelial cells of veins, lungs, and mast cells. It causes the maturation of dendritic cells and the production of IL-4, IL-5, and IL-13 from T cells (7). Numerous receptors in the respiratory system are known as pathogen recognition regulators (PRRs) due to the body's ongoing exposure to pathogenic agents and particles (3, 4). Toll-like receptors (TLRs) are crucial PRRs forming a unique protein family in vertebrates. They mediate the detection of microbial threats, initiating intracellular signaling pathways that activate NF- $\kappa$ B and produce inflammatory cytokines (3, 5, 6).

The primary surface receptors of lung epithelial tissue are TLR2/TLR4. When they signal, several cytokines, including IL-25, IL-33, and TSLP, are released, which can activate Th2 cell-related pathways by releasing IL-5 and IL-13 (3, 4). Their ability to detect the specific pathogen-associated molecular patterns of *Aspergillus* conidia involves the expression of PRRs, and the leading families of these receptors are the TLRs and the lectin receptors. TLR2 and TLR4 have been reported to mediate the recognition of various cell wall components of *Aspergillus* (7), and dectin-1, a C-type lectin receptor, is the major PRR involved in the recognition of  $\beta$ -glucans (8). The involvement of TLRs in the pathogenesis of allergic diseases results from the biological function they play in the

activation and regulation of the immune response. However, the exact role of these receptors remains controversial. Whereas numerous epidemiological studies mainly indicate a protective effect against microbial exposure, experiments show that innate immune stimulation via TLRs may be involved in both the development of and protection against allergic diseases (3-5).

As the majority of the patients suffering from fungal sensitization are severe asthmatics, inhaled corticosteroids and frequent courses of oral corticosteroids are used to control asthma and contribute to alleviating allergic symptoms. Corticosteroids are primarily used to treat allergic asthma and fungus allergies. In addition to having known side effects, corticosteroids can temporarily stop the disease's symptoms. Therefore, it's critical to identify strategies for avoiding fungal sensitivity, such as modifying the host's defenses or using biological substances (1, 9). In recent years, several studies have been conducted on natural resources to find sources rich in antioxidants and anti-inflammatories and the role of consuming these compounds in protecting the body against damage caused by oxidative stress. Phenolic secondary metabolites or polyphenolic compounds partly explain the therapeutic effects of plant sources. Moreover, polyphenol compounds have no harmful effects due to their natural biocompatibility and safety (10, 11). One could describe Pomegranate Seed Oil (PSO) as a potent source of antioxidants and anti-inflammatories (12). PSO has a high amount of phenolic compounds, which suggests potent antioxidant and anti-inflammatory properties (13, 14).

Attention to new drug delivery systems, such as nanostructured carriers for anti-inflammatory properties and prevention of allergies, has increased considerably (15). PSO has diverse bioactivities (16). Considering the numerous potentialities of PSO, it is relevant to study the incorporation of this oil in an effective and stable system for its administration (17). With these

interpretations, nano-emulsions (NEs) are very attractive colloidal systems to use the anti-inflammatory potential of PSO (17). Additionally, studies on NEs have been conducted to improve lipophilic compounds' water solubility, drug bioavailability, and labile substance stability. Oil droplets are dispersed in an external aqueous phase in kinetically stable NE systems, which use a thin layer of stabilizer (18). The smaller droplet size of nano-emulsions makes the formulations less dense and more transparent than traditional emulsions<sup>24</sup>. Furthermore, due to droplet size reduction, nano-emulsions have been studied to increase drug bioavailability, enhance penetration, improve the water solubility of lipophilic compounds, and ameliorate stability of denatured materials (18, 19).

Considering all the benefits of NEs along with the anti-inflammatory and therapeutic benefits of PSO in allergic diseases related to fungi, The purpose of The present study is to investigate how PSO nano emulsion affects the PRRs (TLR2/TLR4) gene expression. This assay was performed in the human lung epithelial cell line (A549) that was sensitized with *A. alternata* cell extract.

## Materials and Methods

### *Preparation of A. alternata cytosolic extract and Protein measurement*

*A. alternata* (ATCC 6663), which was kept under standard conditions in the mycology laboratory of Tehran University, Iran, was used. Similar to Ibarrola et al.'s study (20), *A. alternata* extract was extracted with some changes. Briefly, *A. alternata* young culture was inoculated in Yeast Extract Glucose Broth medium and incubated in a shaker incubator (150 rpm) at 25 °C in the dark. The culture medium was passed through the AP filter (Millipore, Bradford, Massachusetts) after being given the proper turbidity. One hundred microliters of RIPA buffer was added to 3 grams

of dry mass obtained from filtration and homogenized by stirring at 14,000 rpm. The resulting suspension was centrifuged (14000g, at 4 °C, for 15 min.). Finally, the supernatant (Contains cytosolic extract) was removed and stored at -70 °C for further use.

The protein content of an *A. alternata* cell extract was measured using Bradford's technique (21). The blank solution was created using 50 µl of distilled water and 950 µl Bradford's reagent. At 595 nm, the spectrophotometer's absorbance was set to zero. The extract was then diluted with 950 µl of Bradford reagent and read at a wavelength of 595 nm. The amount of protein in the extract was obtained using the standard curve line equation.

### *Preparation of Pomegranate Seed Oil*

Complete and undamaged pomegranate fruits were purchased from local markets in late September (Tehran, Iran). The fruit's maturity was assessed based on its appearance (the colour of external skin and juice). Fruit with flaws (i.e., those with sunburn, cracks, and bruises in the husk) were discarded after buying and being transported to the lab (22). The remaining fruit's seeds were then separated from the juice and carefully cleaned to get rid of any sugars or other adhering substances. Separated seeds were dried (at 35–37 °C) until a constant weight was reached. Dried seeds were pulverized, and particles with size distribution of less than 40-mesh was used for the extraction.

PSO was prepared based on Abbasi et al.'s study using organic solvents and the Soxhlet Extraction method (23). In a Soxhlet apparatus, five grams of the dried seeds were refluxed using two different organic solvents (petroleum benzene and hexane: 155 mL). The solvents were then evaporated at 35 °C in a vacuum oven, and the extracts were dried until a constant weight using a mild flow of nitrogen gas.

According to the method mentioned by Abbasi et al., the chemical compounds of PSO were analyzed using GC analysis. A Varian Star 3400 gas

chromatograph equipped with a capillary column (DB-23, J & W Scientific, 30 m 9 0.25 mm i.d. 9 0.25 lm thick) was used for this purpose. The detector (FID) and injector temperatures were set at 250 and 220 °C, respectively. Nitrogen was used as the carrier gas with an inlet pressure of 33.3 psi. The initial oven temperature was 190 °C and was increased to 220 °C at a rate of 1 °C/min. The peaks were identified by comparing their retention times with those of an authentic standard fatty acid methyl ester mixture (23).

#### *Production of calcium chloride nanoparticles*

In order to form calcium chloride nanoparticles, 20 ml of calcium chloride solution (0.1 M) in pure ethanol was added to oil containing 10% span 80. The mixture was sonicated for 5 min using a titanium probe at the constant frequency of 20 kHz. Then the alcohol was removed using a vacuum oven at 40 °C (24).

#### *Preparation and characterization of nano-emulsions*

In the present study, alginate nanospheres containing PSO were prepared based on the water-in-oil emulsification method proposed by Paques et al. (25) with some modifications. Briefly, an alginate solution containing PSO with the final alginate:PSO ratio of 2:1 was gradually added to an oil phase containing 10% Span 80 as the surfactant. Subsequently, ultra homogenization was used (11500 rpm for 10 min) to form water in oil nano-emulsion. Calcium chloride nanoparticles in oil were then added to the system, resulting in gelation of the alginate. For external gelation, alginate is often dripped into a cation bath, such as a calcium chloride solution (24). The ratio of alginate to calcium chloride nanoparticles was 1:6. After carefully washing with acetone and removing the oil phase (by centrifugation at 10000 rpm for 5 min), the small milky pellet of materials (PSO-loaded NEs) was obtained. Finally, the

prepared PSO-loaded NEs were re-suspended by deionized water.

#### *Characterization and physical stability of PSO-loaded NEs*

The particle size of PSO-loaded NEs was determined by laser light scattering method (26) using Brookhaven zetaplus, USA. Also, the Polydispersity Index (PDI) and zeta potential ( $\zeta$ -potential) were measured as an indicator of the size distribution and stability of particles in the colloid system, respectively (27, 28). The SEM image of the optimal PSO-loaded NE particles was conducted to evaluate the surface morphology and shape of the sample. The samples were stored at 4 °C and 90% relative humidity.

#### *Determination of encapsulation efficiency*

The encapsulation efficiency (EE) value was calculated by measuring the extract's total phenolic compounds (TPC) before and after loading in alginate nanospheres (29). For the measuring of TPC after loading, 100 mg of nanoparticle was dispersed in 1 ml ethanol and deionized water (60:40). The mixture was then vortexed for 5 min and filtered by a 0.45  $\mu$ m filter. The given equation determined the EE:

$$EE (\%) = \frac{TPC \text{ of PSO before loading} - TPC \text{ of PSO after loading}}{2TPC \text{ of PSO before loading}} \times 100$$

#### *A549 cell culture and treatment*

The alveolar epithelial A549 cell line was obtained from the American Type Culture Collection (ATCC number: CCL-185). A549 cells were cultured in a complete cell culture medium containing 89% RPMI 1640 Medium with GlutaMAX<sup>TM</sup>-1 and 25 mM HEPES, 10% fetal bovine serum and 1% penicillin (5000 U/ml)-

streptomycin (5000 µg/ml), and were kept in a humidified atmosphere at 37 °C and 5% CO<sub>2</sub>. Before reaching 90% confluence, cells were subculture using Trypsin (500 mg/l) – EDTA (200 mg/l) solution. Cells were seeded in 6-well plates at  $0.5 \times 10^6$  cells/(ml well) complete cell culture medium for 24 h before exposure to the test substance (30). Cells were treated/stimulated with free *A. alternata* cytosolic extract, *A. alternata* extract with PSO, *A. alternata* extract with PSO-loaded NEs, free nanoparticles, and free PSO, or they were left untreated as a control. Cells were incubated at 37 °C with 5% CO<sub>2</sub> for 16-18 hours. Following treatment, the supernatants were collected, and debris was removed by centrifugation before storing at –80 °C. The cells were then harvested and washed twice with DPBS before RNA extraction. TLR2 and TLR4 mRNA expression levels were examined using real-time RT-PCR. The reproducibility of certain observations was examined in the epithelial A549 cell line.

#### *RNA Preparation and real-time RT-PCR*

Total RNA was purified using the RNX-Plus Total RNA Isolation Kit (SinaClon, Iran), and DNase digestion was performed with DNase I Amplification Grade (SinaClon, Iran). cDNAs were synthesized from 1 µg of purified RNA samples using a cDNA Synthesis Kit (SinaClon, Iran) according to the manufacturer's protocol. The reaction was incubated at 45 °C for 60 minutes and was then stopped by heating to 85 °C for 5 minutes. The real-time RT-PCR reaction mixture contained 1 µl of cDNA, 12.5 µl of Master Mix (SinaSYBR Green HS-qPCRMix, SinaClon, Iran) with HS-Taq DNA polymerase gene expression assays for the target genes (as listed in Table 1). The real-time RT-PCR reactions were prepared to a final volume of 20 µl with sterile water. Amplification and detection of specific products were conducted using the QIAGEN Real-Time PCR Detection System (Rotor-Gene Q). The protocol for real-time

RT-PCR was as follows: Denaturation by a hot start at 95 °C for 10 minutes. Followed by 40 cycles of a two-step program: Denaturation at 95 °C for 15 seconds. Annealing/extension at 60 °C for 1 minute.

#### *Statistical Analysis*

To investigate the effects of various treatments on the expression of TLR2 and TLR4 genes in A549 cells, experimental data were first collected and preliminary analyses were performed. The average and standard error (SE) for each group were calculated to understand the data distribution. Given the non-normal distribution of the data, the Kruskal-Wallis H, a non-parametric test, was employed. The Kruskal-Wallis test assessed whether there were significant differences among the various groups. To visualize the data and the effects of the treatments, both radar and bar charts were generated using Python. Radar charts provided a comparative visual analysis of gene expression levels for TLR2 and TLR4 across different treatment groups, with concentric circles representing fold-change levels. The Kruskal-Wallis test and the generation of the charts were performed using the scipy, pandas, scikit\_posthocs, and matplotlib Python libraries.

## **Results**

#### *Protein concentration of A. alternata extract and PSO Chemical composition*

The amount of protein present in the cytosolic extract of *A. alternata* was obtained in three replicates with an average of 4330 µg/ml. The compositions of PSO are presented in Table 2.

#### *Particle size and size distribution of NEs*

The three-dimensional image of the optimal PSO-loaded alginate nanospheres was shown in

**Table 1.** Real-time RT-PCR Primers.

Gene	Primer (5' to 3')	Primer Melt Temperature, °C	Accession No.
TLR2	TGCTGCCATTCTCATTCTTCTG	60	NM_001318796.2
	AGGTCTTGGTGTTCATTATCTTCC	62	
TLR4	CCAGCCTCCTCAGAAACAGA	60	NM_138554.5
	TCCCTCCAGCAGTGAAGAAG	60	
GAPDH	CCACTCCTCCACCTTTGACG	63	NM_001289745.3
	CCACCACCCTGTTGCTGTAG	63	

**Table 2.** Chemical composition of PSO in the present study.

Compositions	PSO (% w/w)
Triglycerides	93
Diglycerides	2.4
Monoglycerides	0.5
Free fatty acids	0.9
Polymers	1.9
Total composition (%)	98.7
Fatty acid analysis (%)	
C16:0 stearic acid	2.9
C18:0 palmitic acid	2.5
C18:1 oleic acid	5.8
C18:2 linoleic acid	6.9
CLNA*	81.9
Total fatty acid analysis (%)	99.6

\*Conjugated linoleic acid

**Table 3.** The results of Kruskal-Wallis Test in the present study.

Test Parameters	Test Statistics	
	TLR2	TLR4
Kruskal-Wallis H	15.97	16.08
df <sup>a</sup>	4	4
Asymp. Sig.	.000694	.00661

a Degree of freedom.

Figure 1, and the particles had a dense spherical structure.

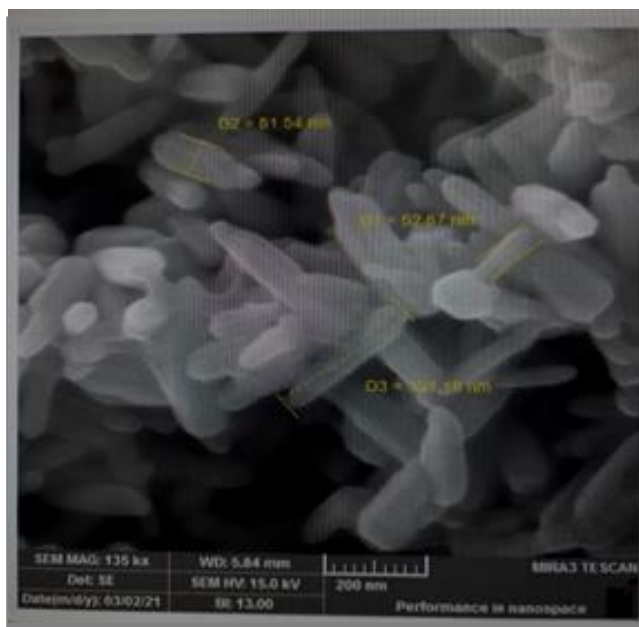


**Fig 1.** SEM image of morphological study of NEs (magnification: 4000×).

#### Characterization of PSO-loaded NEs

In terms of the main parameters measured to characterize PSO-loaded NEs after purification, the mean particle size was  $209.4 \pm 0.6$  nm. The PDI was  $0.0124 \pm 0.022$ , the  $\zeta$ -potential was  $56.42 \pm 0.22$  mV, and the EE percentage was  $83.66 \pm 0.53$ , with  $\pm$  representing the standard deviation ( $n = 3$ ).

#### Statistical analysis

According to Table 3, the Kruskal-Wallis test results indicated significant differences in the expression of TLR2 and TLR4 genes among the different treatment groups. For TLR2, the H-statistic was 15.97 with a p-value of 0.00694, indicating a significant difference between the groups ( $p < 0.05$ ). Similarly, for TLR4, the H-statistic was 16.08 with a p-value of 0.00661, confirming a significant difference among the

treatment groups ( $p < 0.05$ ). These results suggest that the type of treatment had a considerable impact on the expression of TLR2 and TLR4 genes in A549 cells.

#### Gene expression changes in A549 cells

Based on the average values for TLR2 gene expression, the data shows that all the treatment groups exhibited an increase compared to the control group. The *A. alternata* extract with PSO (P+ALT) had the most potent effect, causing a 4.82-fold increase in TLR2 expression. The free PSO (P) and the free NEs (NP) also led to substantial increases of 3.92-fold and 2.93-fold, respectively. The *A. alternata* cytosolic extract (ALT) and the *A. alternata* extract with PSO-loaded NEs (NP+ALT) had more moderate effects, increasing TLR2 expression by 2.26-fold and 2.50-fold, respectively.

Regarding the TLR4 gene expression, the results show a more complex picture. While the ALT led to a 2.29-fold increase in TLR4 expression, the treatments containing PSO, either alone (P) or in combination with P+ALT or NP+ALT, decreased TLR4 expression. Specifically, the P+ALT and NP+ALT treatments caused 0.45-fold and 0.61-fold decreases, respectively, which are notable reductions compared to the control. The free NP also led to a moderate decline of 0.95-fold in TLR4 expression.

When comparing the results for TLR2 and TLR4, it is clear that the treatments had distinct effects on the two receptors. While all the treatments increased TLR2 expression to varying degrees, the treatments containing PSO, either alone or in combination, were particularly effective in reducing the expression of TLR4. This suggests that the PSO-based treatments may have a more selective or targeted effect on the TLR4 pathway compared to the TLR2 pathway in the A549 cell line.

Figure 2 presents a comparative analysis of the gene expression levels of TLR2 and TLR4 across different treatment groups. The data shows a clear

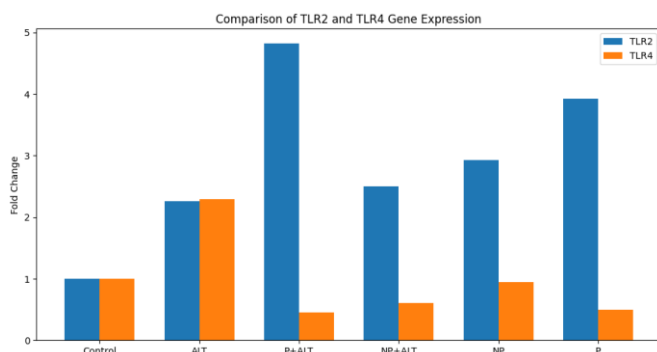


**Fig 2.** Differential Effects of Treatments on TLR2 and TLR4 Gene Expression.

distinction in the effects of the treatments on these two Toll-like receptors. For TLR2 expression, all the treatment groups exhibited an increase compared to the control, with the P+ALT treatment having the most significant impact ( $p < 0.05$ ), leading to a nearly 5-fold increase. The P (free PSO) and NP groups also showed substantial increases in TLR2 expression, whereas the ALT and NP+ALT treatments had more moderate effects. In contrast, the TLR4 expression patterns were more complex. While the ALT treatment led to a 2.29-fold increase in TLR4 expression, the treatments containing PSO, either alone (P) or combined with *A. alternata* extract (P+ALT) or NP+ALT, decreased TLR4 expression. Notably, the P+ALT and NP+ALT treatments caused the most significant reductions, with around 0.45-fold and 0.61-fold decreases, respectively. These results suggest that the PSO-based treatments have a more selective or targeted effect on the TLR4 pathway, suppressing its expression while enhancing TLR2 expression in the A549 cell line.

Figure 3 provides a comprehensive visual analysis of the comparative effects of different treatments on the gene expression of TLR2 and TLR4 in A549 cells. The concentric circles represent the fold-change levels, with the outermost circle indicating a 5-fold change. The chart clearly shows that the P+ALT treatment combined with P+ALT had the most pronounced

and balanced effect on the two receptors. It significantly increased TLR2 expression while substantially decreasing TLR4 expression, suggesting a selective modulation of these pathways. Similarly, the NP+ALT treatment, involving PSO-loaded NEs combined with ALT, and the NP treatment, using free nanoparticles, exhibited a comparable pattern, although with less extreme changes compared to the P+ALT group. In contrast, the ALT treatment, using only the *A. alternata* cytosolic extract, led to increases in both TLR2 and TLR4 expression. At the same time, the control group showed the lowest levels of expression for both receptors.

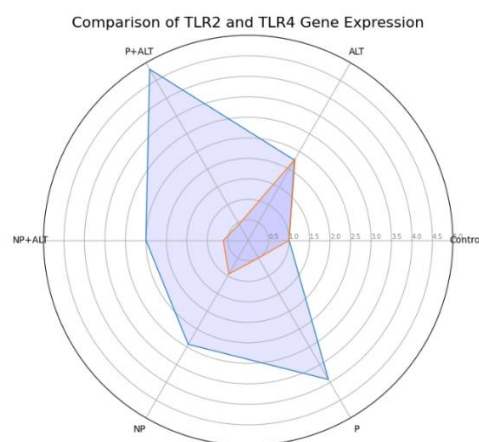


**Fig 3.** Comparative Radar Analysis of TLR2 and TLR4 gene expression patterns in A549 cells under various treatments.

## Discussion

The findings from the present study on the expression of TLR2 and TLR4 genes in response to ALT, free PSO, and PSO-loaded NE treatments are intriguing and provide valuable insights for broader concepts and future research on these therapeutic agents. In the present study, all treatment groups showed increased TLR2 expression compared to the control group, with the P+ALT causing the most significant increase. The PSO alone (P) and NP also led to substantial



increases. Other combinations, such as ALT and NP+ALT, showed moderate effects. These results align with several studies indicating that certain plant extracts and natural compounds can enhance TLR2 expression. Schink et al. (2018) examined the effects of herbal extracts on toll-like receptors (TLRs), particularly TLR2 and TLR4. They screened 99 ethanolic extracts and identified 28 with anti-inflammatory properties, noting that these extracts impacted both TLR2 and TLR4 signaling pathways (31, 32).

Researchers investigated the effects of various plant extracts on TLR2 and TLR4 signaling pathways using cell lines. Echinacea purpurea reduced TLR2 and TLR4 activation, leading to decreased pro-inflammatory cytokine production. *Glycyrrhiza glabra* (licorice) inhibited TLR4-mediated NF- $\kappa$ B activation. *Curcuma longa* (turmeric) suppressed both TLR2 and TLR4 responses. These findings suggest that these extracts have potential as anti-inflammatory agents (32, 33). Green tea polyphenols (catechins) were studied for their impact on TLR2 and TLR4 activation. The results showed that epigallocatechin gallate (EGCG), a major catechin in green tea, inhibited TLR4-induced inflammation by blocking NF- $\kappa$ B signaling. Additionally, EGCG modulated TLR2 responses, indicating a dual effect on both receptors (34). In addition to the anti-inflammatory properties of PSO, incorporating it into nanoscience-based delivery systems (PSO-loaded NEs) significantly enhances its effects. The increased TLR2 expression observed in the present study, particularly with PSO-based treatments, is consistent with these findings, underscoring the potential of these compounds in immune modulation.

The current study presents a more complex picture of TLR4 expression. While the ALT increased TLR4 expression, treatments containing P, P+ALT, and NP+ALT decreased TLR4 expression. Contrary to the upregulation observed for TLR2, the reduction in TLR4 expression with

PSO treatments could suggest a differential regulatory mechanism. Similar outcomes were reported by Hong Byun et al. (2010), who observed that certain plant-derived compounds could selectively downregulate TLR4 expression, potentially mitigating inflammatory responses (35). Additionally, Du et al. (2019) demonstrated that PSO could suppress TLR4-mediated signaling pathways, reducing inflammation in epithelial cells. Unlike the present study, which used nano-emulsified PSO, Du et al.'s research focused on pomegranate peel polyphenols without nano-emulsification (36). These studies support the present findings, indicating that PSO may exert an anti-inflammatory effect by explicitly targeting and reducing TLR4 expression.

The differential effects of the treatments on TLR2 and TLR4 expression highlight a nuanced regulatory mechanism. While all treatments increased TLR2 expression, the PSO-based treatments selectively decreased TLR4 expression. This selective modulation is particularly noteworthy, as it suggests potential therapeutic applications where enhancing TLR2-mediated immune responses while suppressing TLR4-mediated inflammation could be beneficial. The P+ALT combination's balanced effect, significantly increasing TLR2 while substantially decreasing TLR4, points to its potential as a dual modulator of these pathways.

The findings of this study indicate that the *A. alternata* extract sensitizes the A549 cell line by upregulating TLR2 and TLR4 expression, corroborating previous research that highlights the sensitizing properties of this pathogen. *A. alternata* is widely recognized for its allergenic components found in the cell wall and cytoplasm of its conidia and hyphae, which are known to cause respiratory allergic disorders. In a 2010 study, Moosavi et al. demonstrated that exposure to the extract and spores of *A. alternata* leads to a rapid and substantial increase in IL-4 and IL-3 production. These findings confirmed the sensitizing nature of the fungus, with these

cytokines being linked to respiratory histopathological changes (37). Various studies have placed *A. alternata* cytosolic extract in the vicinity of the A549 cell line for multiple purposes, including Murai et al. in 2015, Tapfuma et al. in 2019, and Ashoka et al. in 2023. The method used in the present study was similar to the mentioned studies (38-40).

In the present study's GC analysis of PSO, compounds were identified that are consistent with those found in other research, such as those by Mohamed et al. (2020), Rahnemoon et al. (2021), Meerts et al. (2009), Al-Zoreky et al. (2009), and Yang et al. (2015) (16, 27, 41, 42). The PSO fatty acid composition evaluated by GC showed that the massive component of fatty acid was CLNA (81.9%, w/w). CLNA are naturally occurring fatty acids with multiple biological properties, including regulating metabolic, proliferative, and immune processes. Various studies have demonstrated the role of CLNAs in resolving asthma-related reactions. For instance, MacRedmond et al. reported that CLNA was well tolerated as an adjunct to usual care in overweight individuals with mild asthma and improved key measurement indicators (43).

Many studies have generally shown that the average diameter of nanoparticles varies depending on the compounds used in the formulation and the preparation method (44, 45). In the current study, the size of the nanospheres was measured, and the results showed that their average diameter was 209.4 nm with a very small standard deviation of  $\pm 0.6$  nm. This indicates a high level of precision in the measurements and suggests that the nanospheres were consistently uniform in size. The average diameter value provides important information about the physical properties of the nanospheres, which can influence their behavior, stability, and functionality in various applications, such as drug delivery, diagnostics, or materials science. The uniform size distribution can be critical for ensuring predictable performance and reproducibility in these

applications. Rahnemoon et al.'s study found that the smallest particle size was achieved when using a 6:1 ratio of alginate to  $\text{CaCl}_2$  (27).

When there's an excess of alginate compared to  $\text{CaCl}_2$ , there may not be enough calcium ions available to interact with the hydroxyl groups of alginate. This imbalance can lead to increased aggregation and larger particle sizes. While there's limited research on the role of  $\text{CaCl}_2$ /alginate ratios in characterizing alginate nanospheres, the impact of alginate and  $\text{CaCl}_2$  concentrations has been studied. For instance, Sangeetha et al. (2010) formulated sodium alginate nanospheres containing the drug ofloxacin. They used a ratio of 19:1 between alginate sodium (0.1% w/v) and  $\text{CaCl}_2$  (18 mM), with an optimum drug loading concentration of 20  $\mu\text{g/ml}$ . Their study found an average particle size of  $656.6 \pm 0.28$  nm and a drug loading capacity of 33.2%, which decreased as the drug level increased. They observed better capacity and faster formation rates at relatively lower drug concentrations (46). In another study in 2017, alginate nanoparticles containing curcumin were prepared using alginate (0.5% w/v), resulting in particle sizes of 78.8 nm and a loading efficiency of 13.35% (47). However, contradictory findings were reported in another study evaluating the effect of different alginate and  $\text{CaCl}_2$  concentrations (ranging from 1–2.5% w/v and 1–4% w/v, respectively) on bead characterization. This study found that the alginate concentration was the most influential variable, while changes in the  $\text{CaCl}_2$  ratio had no significant effect on bead size ( $p > 0.05$ ). This observation was attributed to the characteristics of the final alginate polymer, which depended on factors like its source and the sequence of mannuronic and guluronic acid (27, 48).

$\zeta$ -Potential is a crucial parameter influencing the stability of colloids. Colloids with high  $\zeta$ -potential (either negative or positive) are typically electrically stabilized, while those with low  $\zeta$ -potential tend to exhibit coagulation or flocculation tendencies (49). According to the

classification by Greenwood and Kendall, colloids are considered to have good stability if their  $\zeta$ -potential falls within the range of 40 to 60 mV and excellent stability if it exceeds 60 mV (50). In the present study, the  $\zeta$ -potential for PSO-loaded NEs was determined to be  $56.42 \pm 0.22$  mV. According to existing literature, this falls within the satisfactory range and indicates good stability for the colloidal system. A higher value of  $\zeta$ -potential indicates a greater charge on the surface of the nanoparticles. This suggests stronger repulsive interactions between the particles, which contributes to their stability by preventing aggregation or coagulation (51).

In addition to nanoparticle size, EE is a crucial factor in encapsulation procedures. In the present study, the EE percentage was  $83.66 \pm 0.53\%$ . The number of  $\text{CaCl}_2$  particles affects the distribution of calcium on the alginate surface, which in turn influences the properties of the alginate spheres. In a related study examining the effects of  $\text{CaCl}_2$  and alginate ratios on the properties of diphtheria toxoid nanocapsules, 0.025–0.15% w/v of  $\text{CaCl}_2$  was added to a sodium alginate solution. The results indicated that 0.1% w/v of  $\text{CaCl}_2$  was the optimal concentration, yielding the highest production and optimized nanoparticles. The study concluded that insufficient  $\text{CaCl}_2$  could not produce favorable nanoparticles, while concentrations above the optimal level facilitated the aggregation of  $\text{Ca}^{++}$  ions. Furthermore, variations in the ratio of calcium alginate to the encapsulated substance had significant effects on the encapsulation efficiency ( $p < 0.05$ ) (52).

In the present study, a calcium chloride to alginate ratio of 1:6 was used. High ratios of alginate can also lead to a possible loss of active agents, indicating a reduction in the EE. Practically, in a calcium alginate matrix with a stable structure, the number of loading components within the alginate network increases, thereby achieving higher EE (48). In a study by Isa et al. (2016), ciprofloxacin-encapsulated nanoparticles were prepared and characterized.

Their data indicated that increasing the amount of loaded drug resulted in minimal loss, leading to higher EE (53). Comunian et al. studied the encapsulation of PSO, a rich source of bioactive compounds, in a Pickering oil-in-water (O/W) emulsion using WPI microgels and systems with WPI, gum Arabic, modified starch, and maltodextrin. All formulations were stable, resulting in particles with EE ranging from 56.28% to 73.83% and yields ranging from 28.07% to 93.99% (54).

## Conclusion

Our findings are consistent with existing literature on the modulation of TLR2 and TLR4 by Herbal extracts, particularly PSO and plant extracts. The selective upregulation of TLR2 and downregulation of TLR4 by PSO-based treatments suggest a targeted therapeutic potential in inflammatory and immune response modulation. Our results support the potent anti-inflammatory effects of PSO. Furthermore, the benefits of Nano-emulsions were evident, as PSO-loaded NEs demonstrated even better anti-inflammatory effects. The results may help to develop new therapeutic strategies for various inflammatory diseases. Future research should focus on elucidating the underlying molecular mechanisms driving these differential effects and exploring the therapeutic potential of these treatments across multiple disease models.

## Acknowledgements

We extend our sincere gratitude to the Department of Microbiology and Immunology, Faculty of Veterinary Medicine, University of Tehran, for their invaluable support and resources throughout this research. Special thanks to our esteemed colleagues for their insightful discussions and technical assistance, which greatly contributed to the advancement of this study. We also appreciate the administrative staff for their

unwavering support and cooperation. We also thank Dr. Iman Ghasemian Sahebi for his support with statistical analysis.

### Funding Information

This study was conducted with financial support from the University of Tehran.

### Ethics approval and consent to participate

Not needed.

### Conflict of interest

The authors declare that they have no conflict of interest.

### References

1. Cramer R, Garbani M, Rhyner C, et al. Fungi: the neglected allergenic sources. *Allergy* 2014; **69**(2):176-85.
2. Pfavayi Lorraine T, Sibanda Eloy N, Mutapi F. The pathogenesis of fungal-related diseases and allergies in the african population: The state of the evidence and knowledge gaps. *Inte Arch Allergy Immunol* 2020; **181**(4):257-69.
3. Moran G, Arevalo E, Barria M, et al. Expression of Toll-Like receptor 2 (TLR2) and TLR4 in response to *Aspergillus Fumigatus* in murine models of allergic airway inflammation. *Int J Immunol Immunother* 2015; **2**:015.
4. Dang EV, Lei S, Radkov A, et al. Secreted fungal virulence effector triggers allergic inflammation via TLR4. *Nature* 2022; **608**(7921):161-7.
5. Kong Y, Kim M, Jin HS, et al. Association with genetic polymorphism of rs117033348 and allergic disease in korean population. *Biomedical Science Letters* 2021; **27**(3):177-81.
6. Wendlandt EB, Graff JW, Gioannini TL, et al. The role of MicroRNAs miR-200b and miR-200c in TLR4 signaling and NF-κB activation. *Innate Immunity* 2012; **18**(6):846-55.
7. Bellocchio S, Montagnoli C, Bozza S, et al. The contribution of the Toll-Like/IL-1 receptor superfamily to innate and adaptive immunity to fungal pathogens in-vivo. *J Immunol* 2004; **172**(5):3059-69.
8. Netea MG, Brown GD, Kullberg BJ, et al. An integrated model of the recognition of *Candida albicans* by the innate immune system. *Nature Rev Microbiol* 2008; **6**(1):67-78.
9. DuBuske LM. twenty-four-hour duration of effect of intranasal corticosteroids for seasonal allergic rhinitis symptoms: clinical evidence and relevance. *Am J Rhinol Allergy* 2012; **26**(4):287-92.
10. Wardlaw AJ, Rick EM, Pur Ozyigit L, et al. New perspectives in the diagnosis and management of allergic fungal airway disease. *J Asthma Allergy*. 2021; **14**:557-73.
11. Rupani H, Fong WCG, Kyyaly A, et al. Recent Insights into the management of inflammation in asthma. *J Inflammation Res* 2021; **14**:4371-97.
12. Saparbekova A, Kantureyeva G, Kudasova D, et al. Potential of phenolic compounds from pomegranate (*Punica granatum* L.) by-product with significant antioxidant and therapeutic effects: A narrative review. *Saudi J Biol Sci* 2022:103553.
13. Toschi A, Piva A, Grilli E. Phenol-rich botanicals modulate oxidative stress and epithelial integrity in intestinal epithelial cells. *Animals* 2022; **12**(17):2188.
14. Tian M, Bai Y, Tian H, et al. The chemical composition and health-promoting benefits of vegetable oils—a review. *Molecules* 2023; **28**(17):6393.
15. Placha D, Jampilek J. Chronic inflammatory diseases, anti-inflammatory agents and their delivery nanosystems. *Pharmaceutics* 2021; **13**(1):64.
16. Lu LY, Liu Y, Zhang ZF, et al. Pomegranate seed oil exerts synergistic effects with trans-resveratrol in a self-nanoemulsifying drug delivery system. *BPB* 2015; **38**(10):1658-62.

17. Talkar SS, Kharkar PB, Patravale VB. Docetaxel loaded pomegranate seed oil based nanostructured lipid carriers: a potential alternative to current formulation. *AAPS PharmSciTech* 2020; **21**(8):295.
18. Mota Ferreira L, Gehrcke M, Ferrari Cervi V, et al. Pomegranate seed oil nanoemulsions with selective antiangiogenic activity: optimization and evaluation of cytotoxicity, genotoxicity and oxidative effects on mononuclear cells. *Pharm Biol* 2016; **54**(12):2968-77.
19. Mohamed HRH, Tulbah FSA, El-ghor AA, et al. Suppression of tumor growth and apoptosis induction by pomegranate seed nano-emulsion in mice bearing solid Ehrlich carcinoma cells. *Scientific Reports* 2023; **13**(1):5525.
20. Ibarrola I, Suárez-Cervera M, Arilla MC, et al. Production profile of the major allergen Alt a 1 in *Alternaria alternata* cultures. *Annals Allergy Asthma Immunol* 2004; **93**(6):589-93.
21. Bradford MM. A rapid and sensitive method for the quantitation of microgram quantities of protein utilizing the principle of protein-dye binding. *Anal Biochem* 1976; **72**(1):248-54.
22. Fernandes L, Pereira JAC, López-Cortés I, et al. Physicochemical changes and antioxidant activity of juice, skin, pellicle and seed of pomegranate (cv. Mollar de Elche) at different stages of ripening. *FTB* 2015; **53**(4):397-406.
23. Abbasi H, Rezaei K, Rashidi L. Extraction of essential oils from the seeds of pomegranate using organic solvents and supercritical CO<sub>2</sub>. *JAOCs* 2008; **85**(1):83-9.
24. Paques JP, van der Linden E, van Rijn CJ, et al. Preparation methods of alginate nanoparticles. *Adv Colloid Interface Sci* 2014; **209**:163-71.
25. Paques JP, van der Linden E, van Rijn CJM, et al. Alginate submicron beads prepared through w/o emulsification and gelation with CaCl<sub>2</sub> nanoparticles. *Food Hydrocolloids* 2013; **31**(2):428-34.
26. Mohammadi A, Jafari SM, Esfanjani AF, et al. Application of nano-encapsulated olive leaf extract in controlling the oxidative stability of soybean oil. *Food Chemistry* 2016; **190**:513-9.
27. Rahnemoun P, Sarabi-Jamab M, Bostan A, et al. Nano-encapsulation of pomegranate (*Punica granatum* L.) peel extract and evaluation of its antimicrobial properties on coated chicken meat. *Food Bioscience*. 2021; **43**:101331.
28. Basiri L, Rajabzadeh G, Bostan A. Physicochemical properties and release behavior of Span 60/Tween 60 niosomes as vehicle for  $\alpha$ -Tocopherol delivery. *LWT* 2017; **84**:471-8.
29. Saikia S, Mahnot NK, Mahanta CL. Optimisation of phenolic extraction from *Averrhoa carambola* pomace by response surface methodology and its microencapsulation by spray and freeze drying. *Food Chemistry* 2015; **171**:144-52.
30. Auwerx J. The human leukemia cell line, THP-1: A multifaceted model for the study of monocyte-macrophage differentiation. *Experientia* 1991; **47**(1):22-31.
31. Schink A, Neumann J, Leifke AL, et al. Screening of herbal extracts for TLR2- and TLR4-dependent anti-inflammatory effects. *PlosOne*. 2018; **13**(10):e0203907.
32. Buchele V, Abendroth B, Büttner-Herold M, et al. Targeting inflammatory T helper cells via retinoic acid-related orphan receptor gamma t is ineffective to prevent allo-response-driven colitis. *Front Immunol* 2018; **9**:1138.
33. Schink AK. Herbal extracts and their active compounds as modulators of the inflammatory signaling pathways of Toll-like receptor 2 and 4: Dissertation, Mainz, Johannes Gutenberg-Universität, 2018; 2018.
34. Hong Byun E, Fujimura Y, Yamada K, et al. TLR4 signaling inhibitory pathway induced by green tea polyphenol epigallocatechin-3-gallate through 67-kDa laminin receptor. *J Immunol* 2010; **185**(1):33-45.
35. Hong Byun E, Fujimura Y, Yamada K, et al. TLR4 signaling inhibitory pathway induced by green tea polyphenol epigallocatechin-3-gallate through 67-kDa laminin receptor. *J Immunol*

- 2010; **185**(1):33-45.
36. Du L, Li J, Zhang X, et al. Pomegranate peel polyphenols inhibits inflammation in LPS-induced RAW264.7 macrophages via the suppression of TLR4/NF- $\kappa$ B pathway activation. *Food Nutr Res* 2019; 63.
  37. Moosavi Z, Khosravi AR, Sasani F, et al. Evaluation of the correlation between tissue reaction and cytokines patterns induced by *Alternaria alternata* in mice. *Comp Clin Pathol* 2010; **19**(6):607-10.
  38. Ashoka GB, Shivanna MB. Metabolite profiling, in vitro and in silico assessment of antibacterial and anticancer activities of *Alternaria alternata* endophytic in *Jatropha heynei*. *Arch Microbiol* 2023; **205**(2):61.
  39. Tapfuma KI, Uche-Okerefor N, Sebola TE, et al. Cytotoxic activity of crude extracts from *Datura stramonium*'s fungal endophytes against A549 lung carcinoma and UMG87 glioblastoma cell lines and LC-QTOF-MS/MS based metabolite profiling. *BMC Comp Alt Med* 2019; **19**(1):330.
  40. Murai H, Okazaki S, Hayashi H, et al. *Alternaria* extract activates autophagy that induces IL-18 release from airway epithelial cells. *BBRC* 2015; **464**(4):969-74.
  41. Mohamed SS, Fayed AHM. Anti-obesity synergistic effect of pomegranate seed oil (PSO) and arabic gum (AG) in albino rats. *Int J Vet Sci* 2020; **9**(1):84-9.
  42. Al-Zoreky N. Antimicrobial activity of pomegranate (*Punica granatum* L.) fruit peels. *Int J Food Microbiol* 2009; **134**(3):244-8.
  43. MacRedmond R, Singhera G, Attridge S, et al. Conjugated linoleic acid improves airway hyper-reactivity in overweight mild asthmatics. *Clin Exp Allergy* 2010; **40**(7):1071-8.
  44. Khan I, Saeed K, Khan I. Nanoparticles: Properties, applications and toxicities. *Arab J Chemistry* 2019; **12**(7):908-31.
  45. Mogilevsky G, Hartman O, Emmons ED, et al. Bottom-up synthesis of anatase nanoparticles with graphene domains. *ACS Appl Mater Interfaces* 2014; **6**(13):10638-48.
  46. Sangeetha S, Deepika K, Thrishala B, et al. Formulation and in vitro evaluation of sodium alginate nanospheres containing ofloxacin. *Int J Appl Pharm* 2010; **2**(4):1-3.
  47. Maghsoudi A, Yazdian F, Shahmoradi S, et al. Curcumin-loaded polysaccharide nanoparticles: Optimization and anticariogenic activity against *Streptococcus mutans*. *Mater Sci Eng C*. 2017; **75**:1259-67.
  48. Lotfipour F, Mirzaeei S, Maghsoudi M. Evaluation of the effect of CaCl<sub>2</sub> and alginate concentrations and hardening time on the characteristics of *Lactobacillus acidophilus* loaded alginate beads using response surface analysis. *Adv Pharm Bull* 2012; **2**(1):71-8.
  49. Al-Zoreky NS. Antimicrobial activity of pomegranate (*Punica granatum* L.) fruit peels. *Int J Food Microbiol* 2009; **134**(3):244-8.
  50. Greenwood R, Kendall K. Selection of suitable dispersants for aqueous suspensions of zirconia and titania powders using acoustophoresis. *J Eur Ceram* 1999; **19**(4):479-88.
  51. Borumand MR. Preparation and characterization of sodium alginate nanoparticles containing ICD-85 (venom derived peptides). *IJJAS* 2013; **4**(3):534-42.
  52. Sarei F, Dounighi NM, Zolfagharian H, et al. Alginate nanoparticles as a promising adjuvant and vaccine delivery system. *Indian J Pharm Sci* 2013; **75**(4):442-9.
  53. Isa T, Zakaria ZAB, Rukayadi Y, et al. Antibacterial activity of ciprofloxacin-encapsulated cockle shells calcium carbonate (aragonite) nanoparticles and its biocompatibility in macrophage J774A.1. *Int J Mol Sci* 2016; **17**(5):713.
  54. Comunian TA, da Silva Anthero AG, Bezerra EO, et al. Encapsulation of pomegranate seed oil by emulsification followed by spray drying: evaluation of different biopolymers and their effect on particle properties. *Food Bioprocess Technol* 2020; **13**(1):53-66.